Pergamon

Tetrahedron 56 (2000) 9375–9382

TETRAHEDRON

Experimental and Computational Studies on Substituent Effects in Reactions of Peracid–Aldehyde Adducts

Christel Lehtinen,* Vesa Nevalainen and Gösta Brunow

Laboratory of Organic Chemistry, University of Helsinki, P.O. Box 55, FIN-00014, Helsinki, Finland

Received 27 June 2000; revised 4 September 2000; accepted 21 September 2000

Abstract—Liquid phase oxidation of six branched and four linear aldehydes by dioxygen and *m*-chloroperbenzoic acid was studied experimentally. 2-Substituted (α-branched) aldehydes reacted to give formates (via Bayer–Villiger mechanism) whereas the related linear saturated aldehydes were converted to the corresponding carboxylic acids. Formation of both these products can be rationalized via rearrangement reactions of peracid–aldehyde adducts **1**. Computational studies employing DFT methods at the DNPP level with the Spartan program (v5.0) were carried out in order to understand properties of those adducts. Conformational properties of the adducts **1** were found to shed light on the differences observed in the reactions of linear and branched adducts.

Introduction

The liquid phase oxidation of aldehyde by dioxygen has been extensively studied.[1] The general scheme of the free radical mechanism of aldehyde oxidation to carboxylic acids consists of consecutive and parallel elementary stages of chain initiation, propagation, branching and termination[1] as described below (Eqs. (1–4)):

$$\mathrm{RCHO} + \text{initiator} \rightarrow \mathrm{RCO^{\cdot}} \quad (1)$$

$$\mathrm{RCO^{\cdot}} + \mathrm{O_2} \rightarrow \mathrm{RCO_3^{\cdot}} \quad (2)$$

$$\mathrm{RCO_3^{\cdot}} + \mathrm{RCHO} \rightarrow \mathrm{RCO_3H} + \mathrm{RCO^{\cdot}} \quad (3)$$

$$\mathrm{RCO_3H} + \mathrm{RCHO} \rightarrow 2\mathrm{RCOOH} \quad (4)$$

In the final stage of the reaction (Eq. (4)), two molecules (the reactant aldehyde and the newly formed peracid) react[1] to form adduct **1** as shown in Scheme 1. Further decomposition of **1** gives rise to the formation of carboxylic acid (pathway **a**) or formate (pathway **b**). An adduct analogous to **1** is presumably also formed when aldehyde is oxidized with *meta*-chloroperbenzoic acid (*m*-CPBA).

The Baeyer–Villiger rearrangement of **1** (path **a**, migration of hydrogen, Scheme 1) provides, in an ideal case, complete conversion of the precursor aldehyde to the corresponding acid whereas the rearrangement of the alkyl moiety of **1** (pathway **b**) leads to the formation of a 1:1 mixture of formate and acid. Therefore, for the purposes of acid production, the latter pathway (**b**) is clearly inferior, and process optimization is needed to avoid it. However, although in some cases (e.g. when treating aromatic aldehydes with peracids)[2] pathway **b** is known to be highly favored, only a few reports[3–5] related to the conversion of aliphatic aldehydes to formates have been published. For example, an α-oxygen substituted aldehyde[3] and β-lactam[4] have been converted to the corresponding formates by oxidation with *m*-chloroperbenzoic acid. Recently, Barrero et al. have reported conversion of α-branched terpenic aldehydes to the corresponding formates (also with peracid treatment).[5]

Although both pathways (**a** and **b**, Scheme 1) can be better understood in the light of the well known *trans*-relation of the leaving and migrating groups (Fig. 1), the properties of **1** appear to be rather poorly understood. Therefore, we have undertaken a comparative experimental and computational study on adducts **1** derived from linear and branched aldehydes. Effects of branching were studied experimentally with 2-ethylhexanal, 2-ethylbutanal and cyclohexanecarboxaldehyde (α-branched) and 3-methylbutanal (β-branched). Besides these, straight chain aldehydes, such as octanal and pentanal, aromatic 2- and 3-phenylpropionaldehyde, Cinnamaldehyde and olefinic *trans*-2-decenal were investigated experimentally. Hexanal and 2-ethylbutanal were chosen as models of linear and branched aldehydes for the computational study of **1**.

Synthetic Results and Discussion

The experimental results are presented in Table 1. Results of the computational studies are summarized in Figs. 2 and 3. In the absence of solvent (with O_2 as oxidant) about 25% of

* Corresponding author. Tel.: +358-40-7032979; fax: +358-40-19140366; e-mail: christel.lehtinen@helsinki.fi

0040–4020/00/$ - see front matter
PII: S0040-4020(00)00908-X

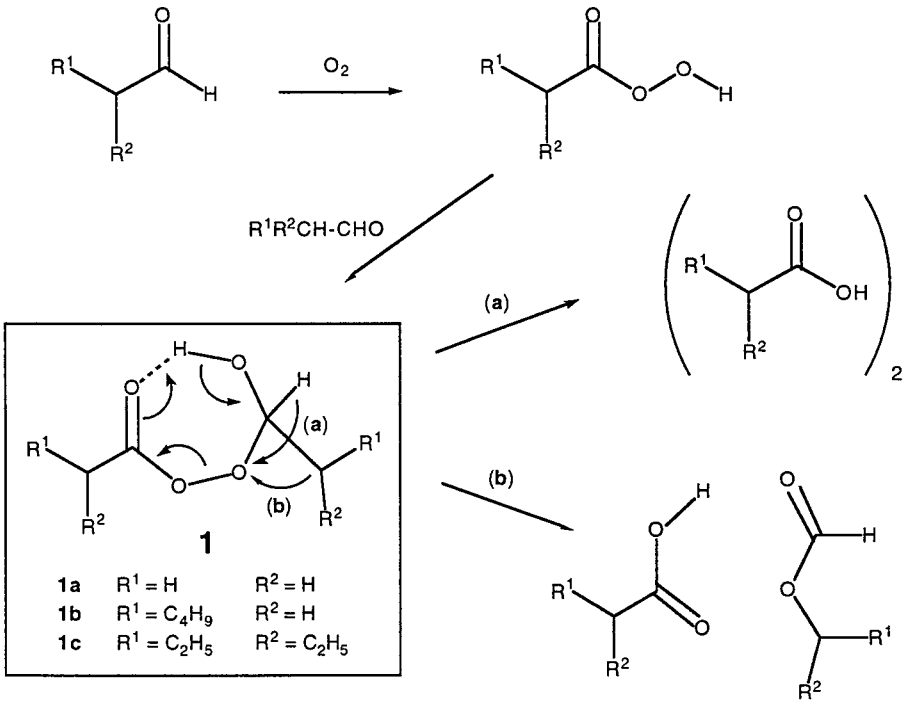

Scheme 1. Oxidation of aldehydes to the corresponding acid via reactions of peracid–aldehyde adduct **1**. Pathway **a** leads to the formation of pure acid at best whereas pathway **b** leads to a 1:1 mixture of the acid and formate.

adducts formed from the α-branched aldehydes, such as 2-ethylhexanal and 2-ethylbutanal, reacted (entries 1–5, Table 1) via carbon chain migration (pathway **b**, Scheme 1). When $C_2H_4Cl_2$ was used as a solvent, the contribution of pathway **b** reached almost one half of the total conversion of the starting material (formate/acid ratio 0.43, entry 2, Table 1). When using *m*-CPBA as oxidant with 2-ethylhexanal migration of the alkyl moiety (pathway **b**, Scheme 1) was preferred over that of hydrogen (pathway **a**) in the ratio of 79/21 (entry 1, Table 1). In the case of 2-ethylbutanal the corresponding ratio was 73/23 (entry 4, Table 1).

Cyclohexanecarboxaldehyde converted to formate slightly less than 2-ethylhexanal and 2-ethylbutanal (entries 21–23, Table 1). The adduct of *m*-CPBA with cyclohexanecarboxaldehyde (analogous to **1**, Scheme 1) decomposed to give 55% formate and 44% acid (entry 21, Table 1) indicating that the lower flexibility of carbon skeleton of cyclohexanecarboxaldehyde (as compared with the more flexible open-chain structure of 2-ethylhexanal and 2-ethylbutanal) might retard the alkyl migration. A phenyl group at the α-position directed the reaction more efficiently to the formate than did the ethyl group (entries 18–20, Table 1). Although initiation of the free radical mechanism did not occur in the case of O_2 oxidation of 2-phenylpropionaldehyde (entry 19–20, Table 1), the aldehyde was converted almost completely to the formate when *m*-CPBA was used as the oxidant (entry 18, Table 1).

Results shown in Table 1 indicate that the presence of α-branching in the carbon chain of the reacting aldehyde clearly correlates with formate production (pathway **b**). Even when a peracid, such as *m*-CPBA, was present in the reaction mixture from the beginning of the oxidation procedure of straight chain aldehydes, such as octanal or pentanal, formate was not detected. Indeed, all straight chain aldehydes converted almost completely to the corresponding carboxylic acids (entries 6–11, Table 1). Furthermore, branching in the α-position appears to be crucial for the formate production, as β-branched 3-methylbutanal (entries 12–14, Table 1) and 3-phenylpropionaldehyde (entries 15–17, Table 1) reacted in the same way to give the corresponding acid as octanal and pentanal.

The effect of a double bond in the α-position was tested with cinnamaldehyde and *trans*-2-decenal using air or O_2 as oxidant. Cinnamaldehyde did not react under standard conditions (entry 24, Table 1), but when arising the

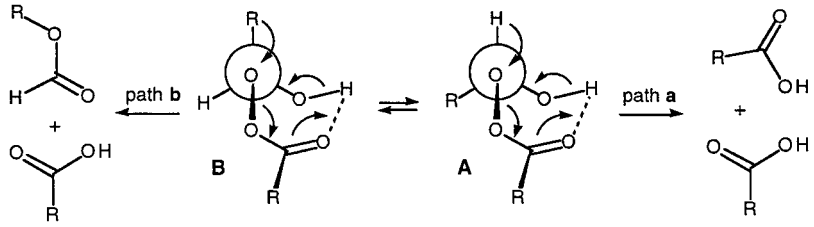

Figure 1. Decomposition of epimers **A** and **B** of peracid–aldehyde adducts **1**. The migrating counterpart is *trans* to the leaving carboxylate about the C–O bond along which the Newman projections are drawn.

Table 1. Oxidation of various aldehydes with air, *m*-CPBA or O_2 (reactions were performed (unless noticed otherwise) as follows: at room temperature; reaction time 1 h 30 min. to 2 h; stirring rate 1000–1250 rpm; air bubbling rate 34 ml/min; the amount of aldehyde ~13 mmol; the *m*-CPBA/aldehyde ratio 1.2/1; 10 ml co-solvent. In the absence of the co-solvent the amount of aldehyde was 36 mmol)

Aldehyde	Entry	Oxidant	Solvent	Product distribution				Formate/acid ratio in the product
				Aldehyde	Formate	Acid	Other[a]	
2-Ethylhexanal	1	*m*-CPBA	CH_2Cl_2	Trace	79	21	Trace	3.76
	2	Air	$C_2H_4Cl_2$	51	13	30.5	5.5	0.43
	3	Air	–	3.5	12	80	4.5	0.15
2-Ethylbutanal	4	*m*-CPBA	CH_2Cl_2	4	73	23	–	3.30
	5	Air	–	3	13	80	4	0.16
Octanal	6	*m*-CPBA	CH_2Cl_2	–	–	100	–	–
	7	O_2	$C_2H_4Cl_2$	91	–	9	–	–
	8	Air	–	9.5	–	90.5	–	–
Pentanal	9	*m*-CPBA	CH_2Cl_2	–	–	100	–	–
	10	O_2	$C_2H_4Cl_2$	70	–	28	2	–
	11	O_2	–	10.5	–	85	4.5	–
3-Methylbutanal	12	*m*-CPBA	CH_2Cl_2	22	–	78	–	–
	13	O_2	$C_2H_4Cl_2$	46.5	–	48.5	5	–
	14	O_2	–	11.5	–	80	8.5	–
3-Phenylpropionaldehyde	15	*m*-CPBA	CH_2Cl_2	–	–	100	–	–
	16	O_2	$C_2H_4Cl_2$	52.5	–	47.5	–	–
	17	O_2	–	26	–	74	–	–
2-Phenylpropionaldehyde	18	*m*-CPBA	CH_2Cl_2	–	~96	~2	Trace	48
	19	O_2	$C_2H_4Cl_2$	~100	–	–	–	–
	20	O_2	–	~100	–	–	–	–
***c*-Hexanecarboxaldehyde**	21	*m*-CPBA	CH_2Cl_2	1	55	44	−1.27	
	22	O_2	$C_2H_4Cl_2$	11	22.5	66.5	–	0.33
	23	O_2	–	18.0	6.5	75.5	Trace	0.09
Cinnamaldehyde	24	Air	–	100	–	–	–	–
***trans*-2-Decenal**	25	Air	–	77	–	21	2	–

[a] Includes also materials of the reaction mixture lost because of evaporaton during air and O_2 oxidations.

temperature after 3 h to 60°C some reactivity was afforded. After 7 h, about 40% of aldehyde had reacted mostly to acid but benzaldehyde and benzoic acid were also formed as decomposition products.

trans-2-Decenal was less reactive than any of the straight chain or α-branched aliphatic aldehydes studied. Under standard conditions about 21% of *trans*-2-decenal was converted in 2 h mostly to the corresponding acid (entry 25, Table 1). Oxidation of *trans*-2-decenal was also performed under more severe conditions: At 60°C and 3.6 bar (airflow 250 ml/min) *trans*-2-decenal reacted almost completely to give *trans*-2-decenoic acid in 2 h. Besides *trans*-2-decenoic acid, small amounts of the fragmentation products nonenol and octanoic acid were also formed.

Decomposition of adduct **1** formed from *trans*-2-decenal or Cinnamaldehyde and the corresponding peracid occurred only by hydrogen migration, indicating that an sp^2 carbon at α-position does not enhance the rate of the reaction along pathway **b** (Fig. 1).

Models and Methods of Computational Studies

The epimeric structures **1a** and **1a′** (with conformers **1′a** and **1′a′**) of the pseudo 7-membered ring system studied computationally are depicted in Fig. 2. Conformations of the $R_{ax.}/R_{eq.}$ group are shown in Fig. 3. Structure **1′a′** is the enantiomer of **1a** (as is **1′a′** the enantiomer of **1a′**).

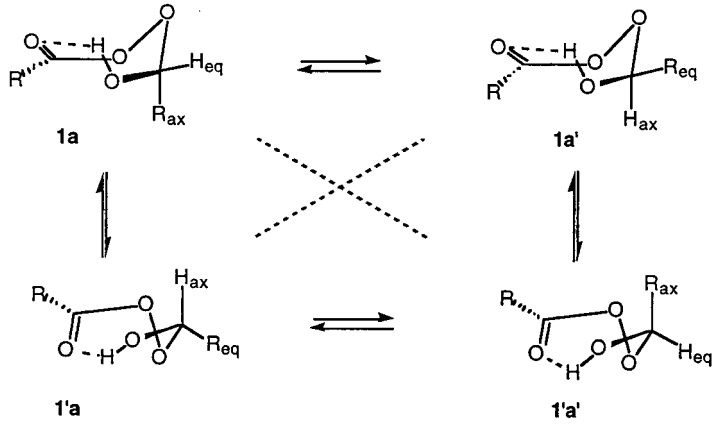

Figure 2. Epimeric intermediates [e.g. **1a** and **1a′** (R=CH_3)] potentially formed when peracid R-CO_3H adds to aldehyde R-CHO. Inversion of the chair of the pseudo-cyclic system of **1a** gives **1′a** that is an enantiomer of **1a′**. Accordingly, similar inversion of **1a′** gives **1′a′** which is an enantiomer of **1a**. These enantiomeric relations are indicated with dashed lines.

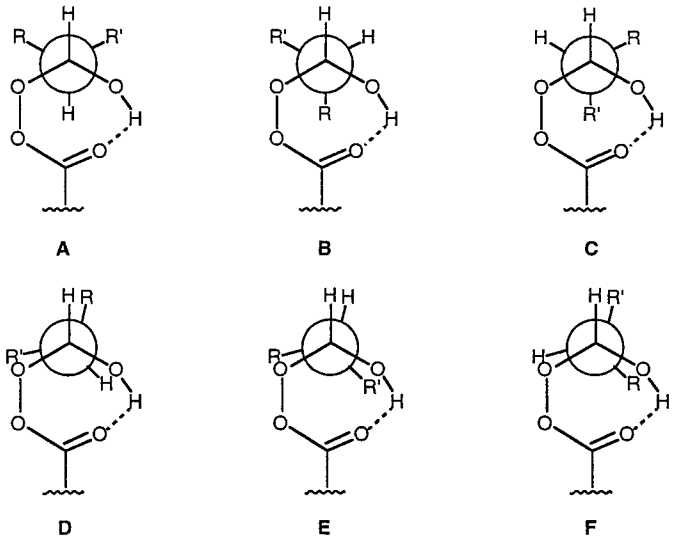

Figure 3. Conformations **A**–**F** of the substituents of the aldehyde moiety of peracid–aldehyde adducts **1b/1b′** (R=*n*-C_4H_9, R′=H) and **1c/1c′** (R, R′=C_2H_5) studied computationally. The substituent of the peracid moiety is omitted for clarity.

For purposes of this study, models of **1** (Fig. 1) were calculated for R=CH_3 (**1a/1a′**, Fig. 2), R=*n*-C_5H_{11} (**1b/1b′**, Fig. 2), and R=$CH(C_2H_5)_2$ (**1c/1c′**, Fig. 2). Six plausible conformations of the substituent R_{ax} and R_{eq} (Fig. 3) were considered in the case of **1b/1b′** and **1c/1c′**. The chain of the substituent R of the C_{CO3H} moiety (Fig. 2) was allowed to stay in a staggered conformation in all optimizations of **1b/1b′**. In the case of **1c/1c′** the C=O bond of C_{CO3H} was allowed to stay in an eclipsed conformation relative to the H atom at the alpha position (i.e. torsion angle O=C–C–H of the C_{CO3H} moiety was close to zero in all conformers of **1c/1c′**). The chain which the two adjacent ethyl groups form when connected by the alpha carbon was also in a staggered conformation in the case of all conformers of **1c/1c′**.

All computational studies were carried out employing DFT methods at the DNPP level with the Spartan[6] program. All structures were fully optimized employing the standard options of the program. Despite the industrial importance of the process of oxidation of aldehydes to carboxylic acids, no previous computational studies on these peracid–aldehyde adducts appeared to be published in the literature.

Table 2. Energies (*E*) and lengths (*r*) of the bonds of the 7-membered pseudo-ring of the optimized structures of **1a**, **1b**, **1c** (equatorial H_{CHO}) and **1a′**, **1b′**, **1c′** (axial H_{CHO})

Struc.[a]	*E* (a.u.)	r^b (C=O)	r^b ($O_{C=O}$–H_{OH})	r^b (O–H)	r^b (O_{OH}–$C_{ald.}$)	r^b ($C_{ald.}$–O_{OO})	r^b (O–O)	r^b (O_{OO}–$C_{C=O}$)
1a	454.70589	1.209	1.852	0.990	1.378	1.415	1.457	1.352
1a′	454.70491	1.209	1.864	0.990	1.380	1.415	1.446	1.353
1b (A)	766.36757	1.210	1.833	0.991	1.376	1.417	1.445	1.349
1b (B)	766.36565	1.211	1.812	0.992	1.377	1.414	1.468	1.345
1b (C)	766.36716	1.210	1.837	0.992	1.378	1.413	1.465	1.349
1b (D)	766.36230	1.211	1.834	0.992	1.377	1.415	1.463	1.349
1b (E)[c]	–	–	–	–	–	–	–	–
1b (F)	766.36085	1.211	1.833	0.992	1.377	1.414	1.467	1.348
1b′ (A)	766.36525	1.210	1.826	0.992	1.380	1.413	1.452	1.351
1b′ (B)	766.36538	1.210	1.852	0.990	1.379	1.416	1.448	1.351
1b′ (C)	766.36580	1.211	1.810	0.993	1.382	1.407	1.456	1.349
1b′ (D)	766.36286	1.210	1.824	0.992	1.380	1.414	1.457	1.350
1b′ (E)[c]	–	–	–	–	–	–	–	–
1b′ (F)	766.36197	1.211	1.823	0.992	1.379	1.413	1.460	1.348
1c (A)	766.36863	1.210	1.858	0.991	1.383	1.407	1.456	1.349
1c (B)	766.36710	1.211	1.847	0.992	1.379	1.414	1.463	1.348
1c (C)	766.36639	1.212	1.826	0.993	1.378	1.412	1.465	1.346
1c (D)	766.36046	1.210	1.881	0.992	1.379	1.413	1.459	1.347
1c (E)[c]	–	–	–	–	–	–	–	–
1c (F)	766.36374	1.210	1.913	0.990	1.381	1.412	1.457	1.352
1c′ (A)	766.36527	1.211	1.848	0.992	1.384	1.411	1.448	1.351
1c′ (B)	766.36570	1.211	1.847	0.991	1.381	1.409	1.446	1.351
1c′ (C)	766.36618	1.211	1.872	0.990	1.382	1.411	1.447	1.352
1c′ (D)	766.35691	1.210	1.896	0.990	1.386	1.411	1.445	1.354
1c′ (E)	766.35497	1.210	1.857	0.990	1.383	1.413	1.448	1.354
1c′ (F)	766.35987	1.212	1.819	0.994	1.379	1.415	1.457	1.349

[a] For **1a**–**c**, the Scheme; for **1x** vs. **1x′** (**x**=**a**, **b** or **c**), Fig. 2; for **A**–**F**, Fig. 3.
[b] Bond lengths (*r*) in Å.
[c] The conformer was found to be unstable.

Table 3. Selected bond (σ) and torsion (γ) angles of the 7-membered pseudo-ring of the optimized structures of **1a**, **1b**, **1c** (equatorial H_{CHO}) and **1a′**, **1b′**, **1c′** (axial H_{CHO})

Struc.[a]	σ[b] (H–$C_{ald.}$–O_{OO})	σ[b] (R–$C_{ald.}$–O_{OO})	γ[b,c] (X–$C_{ald.}$–O–O)	Struc.[a]	σ[b] (H–$C_{ald.}$–O_{OO})	σ[b] (R–$C_{ald.}$–O_{OO})	γ[b,c] (X–$C_{ald.}$–O–O)
1a	97.3	113.5	178.5	**1a′**	109.8	101.9	177.5
1b (A)	97.2	113.4	178.1	**1b′** (A)	109.8	102.4	172.9
1b (B)	96.4	116.0	176.5	**1b′** (B)	110.2	101.9	179.8
1b (C)	97.6	113.6	178.4	**1b′** (C)	110.1	102.2	172.5
1b (D)	96.9	114.1	177.7	**1b′** (D)	109.7	101.6	173.7
1b (E)[c]	–	–	–	**1b′** (E)[c]	–	–	–
1b (F)	96.3	113.8	177.9	**1b′** (F)	109.6	101.0	173.2
1c (A)	97.6	114.8	176.4	**1c′** (A)	110.3	102.9	175.8
1c (B)	96.7	117.4	178.7	**1c′** (B)	110.1	102.7	174.7
1c (C)	96.3	116.9	177.1	**1c′** (C)	110.3	102.4	177.7
1c (D)	95.9	117.5	177.9	**1c′** (D)	109.4	105.3	176.1
1c (E)[c]	–	–	–	**1c′** (E)	109.3	104.9	176.5
1c (F)	97.5	113.8	177.8	**1c′** (F)	110.1	100.9	176.4

[a] For **1a**–**c**, the Scheme; for **1x** vs. **1x′** (**x**=**a**, **b** or **c**), Fig. 2; for **A**–**F**, Fig. 3.
[b] Angles in degrees.
[c] X is the migrating group (either R or H, Fig. 1).

The utility that DFT based methods offer for inspection of compounds containing O–O bonds has been recently illustrated by Freccero, Gandolfi, Sarzi–Amade and Rastelli,[7] who have carried out a thorough computational study on the epoxidation of olefines in the presence of peracids. The energies and the lengths of the bonds of the pseudo cyclic systems of the optimized structures are presented in Table 2 whilst selected bond and torsion angles are shown in Table 3.

Computational Studies—Results and Discussion

Results summarized in Table 2 indicate clearly, that adducts (**1a**, **1b** and **1c**) of which the H_{CHO} atom is in an equatorial position about the pseudo-ring are more stable than their epimers (**1a′**, **1b′** and **1c′**, H_{CHO} atom in an axial position). In the case of acetaldehyde adducts **1a** and **1a′** (R=CH_3, Fig. 2) the former is 2.6 kJ mol^{-1} more stable than the latter (Table 2). In the case of **1b**/**1b′** the related energy difference of the most stable conformers [**1b** (B) and **1b′** (C), Table 2] is 5.8 kJ mol^{-1}. The corresponding energy difference for **1c** (A)/**1c′** (C) is 6.4 kJ mol^{-1}.

The small energy differences between the epimers indicate that both types of adduct (H-equatorial and H-axial, Fig. 2) could be present in a mixture of R-CHO and R-CO_3H when R at the alpha position is either a straight chain or branched chain alkyl group. Interestingly, these energy differences are smaller than the differences between the most stable and the least stable one of conformers (A–F, Fig. 3) of each class of epimers inspected (Table 2). For example, in the case of **1b**, the most stable of the conformers is **1b** (A), which is 17.6 kJ mol^{-1} more stable than the least stable one [i.e. **1b** (F)]. The related energy differences for the other conformers are 10.1 [for **1b′** (C)–**1b′** (F)], 21.5 [for **1c** (A)–**1c** (D)] and 29.4 kJ mol^{-1} [for **1c′** (C)–**1c′** (E)], respectively.

In all cases studied (except **1c′**) conformation E (Fig. 3) was found to be unstable (Table 2). This lack of stability can be easily rationalized by considering repulsion between the R group and one of the free electron pairs of the oxygen adjacent to the carbonyl carbon of the peracid moiety. In the case of **1b** (axial *n*-C_5H_{11}) two almost equally stable conformers (A and C) can be found whereas epimer **1b′** (equatorial *n*-C_5H_{11}) has three conformers (A, B and C) of similar stability (Table 2). Interestingly, whilst epimer **1c** has only one conformer (A) clearly more stable than the others, epimer **1c′** has two (B and C) almost equally stable conformers.

The bond lengths of the optimized structures (Table 2), except that of the hydrogen bond ($O_{C=O}$–H_{OH}), are very similar. The similarity is the closest in the case of the C=O and O–H bonds of which the lengths appear to be almost constant (variation of the values is only 0.002 Å and 0.004 Å). This is somewhat surprising, because the $O_{C=O}$ and H_{OH} atoms form a hydrogen bond, of which the length varies between the values 1.810 Å and 1.913 Å [of **1b′** (C) and **1c** (F)]. As could be expected, the hydrogen bond of the more stable epimer appears to be slightly shorter. For example, the $O_{C=O}$–H_{OH} bond of **1a** is 0.012 Å shorter than that of **1a′** (Table 2). Interestingly, the difference in lengths of the hydrogen bonds does not depend on the increasing bulkiness of the R group (Fig. 2). When the values of the most stable conformers of epimers **1b** (A)/**1b′** (B) and **1c** (A)/**1c′** (C) are compared (Table 2), the $O_{C=O}$–H_{OH} bonds of the more stable epimers (**1b** and **1c**) are found to be 0.23 Å and 0.014 Å shorter than those of the less stable ones (**1b′** and **1c′**). However, there is no general correlation between the stability and the length of the hydrogen bond [e.g. the $O_{C=O}$–H_{OH} bonds of **1b** (A) and **1b** (F) are equally long although the former is 17.6 kJ mol^{-1} more stable than the latter one].

After the hydrogen bond the next most varying bond lengths of the epimers studied is the O–O bond, that appears to vary in the range of 1.445–1.468 Å, respectively. If the most stable conformers of each class of epimers are considered, it can be seen that the lengths of the O–O bonds are 1.445 and 1.448 Å (i.e. almost equal) in the case of linear **1b** (A)/**1b′** (C) but in the case of branched **1c** (A) vs. **1c′** (C) the corresponding lengths are 1.456 and 1.447 Å, respectively. Interestingly, the length of the O–O bond of adduct **1c** (A) is longer than that of **1b** (A) indicating that **1b** (A) could react more easily via pathway **a** (Fig. 1) than **1c** (A). This is consistent with experimental observations. As in the case of the $O_{C=O}$–H_{OH} bond discussed above, there is no general

correlation between the stability and the length of O–O bond. For example, in the case of **1c′** lengths of the O–O bonds of the most stable and least stable one of the conformers [i.e. **1c′** (C) and **1c′** (E)] differ only by 0.001 Å. The lengths of the O_{OH}–$C_{ald.}$, $C_{ald.}$–O_{OO}, O_{OO}–$C_{C=O}$ bonds vary in the following ranges: 1.376–1.386 Å, 1.407–1.417 Å and 1.345–1.354 (i.e. all ≤0.010 Å, Table 2).

As the conversion of adducts **1** to the products (the Scheme) will involve migration of either R or H of the R-CHO moiety of **1** (Fig. 1), the bond angles R–C–O and H–C–O along with the torsion angle X–C–O–O [in which X is the migrating group (i.e. R or H)] could be worth comparing. The values of these angles are presented in Table 3.

When the migration of hydrogen takes place along pathway **a** (Fig. 1) the bond angle H–$C_{ald.}$–O will first approach 90° and then decrease significantly below the level of 90°. Therefore, the smaller the value of this angle in adduct **1**, the more closely its structure resembles the transition state structure of the pathway (**a**, Fig. 1). Among the conformers of **1b** and **1c** (H migrating) the least stable ones are the adducts **1b** (F) and **1c** (D). However, the H–$C_{ald.}$–O bond angle of **1b** (F) is closer to 90° than that of any other of the conformers of **1b**. The same observation can be made in the case of **1c** (D). When the values of the R–$C_{ald.}$–O angle of conformers of **1b′** and **1c′** (R migrating) are compared it can be seen that the values closest to 90° belong to the conformers **1b′** (F) and **1c′** (F) both of which in turn belong to the group of the most unstable conformers. This is consistent with the well known Hammond postulate.

When the H–$C_{ald.}$–O bond angles of adducts **1b** and **1c** (hydrogen should migrate) are compared with those of **1b′** and **1c′** (hydrogen should not migrate) the values of the former group are all clearly closer to 90°. In the same way, when the R–$C_{ald.}$–O bond angles of adducts **1b** and **1c** (R should not migrate) are compared with those of **1b′** and **1c′** (R should migrate), the values of the latter group are all clearly closer to 90°. On the other hand, the H–$C_{ald.}$–O bond angles of adducts **1b** and **1c** (hydrogen should migrate) are about 5–6° smaller than the values of the related R–$C_{ald.}$–O angles of their epimers **1b′** and **1c′** (R should migrate). Therefore, migration of hydrogen (**a**, Fig. 1) should be clearly more favorable than that of R (**b**, Fig. 1). This is consistent with the experimental results (Table 1).

The X–C–O–O [X is the migrating group (i.e. R or H)] torsion angles listed in Table 3 are also revealing when one is trying to understand why formates are formed when α-substituted aldehydes are oxidized but not when the corresponding straight chain aldehydes are treated accordingly. Namely, the X–C–O–O torsion angles of all conformers of epimer **1b′** [except that of **1b′** (B), Table 3] clearly deviate from 180° more (four of the values in the range of 172.5–173.7°) than those of **1b**, **1c** or **1c′** (only two values out of the range 176.4–178.7°). Therefore, the less favorable spatial arrangement of the migrating group in the case of straight chain aldehydes (analogous to **1b**) could inhibit the formation of formates (via pathway **b**, Fig. 1) whereas in the case of α-branched aldehydes both mechanisms (along with pathway **a** and **b**, Fig. 1) could operate giving rise to the formation of formate along with the acid.

One way to inspect the results of the computational study (Tables 2 and 3) is to select structures of which the geometrical parameters show maximum similarity with those of the transition state of the reaction. This type of comparison can be carried out although the exact transition state had not been determined because the direction of the change of the structural parameters is known, as illustrated in Table 4. In a maximum similarity structure the shortening bonds belong to the group of the shortest bonds and the lengthening bonds belong to the group of the longest bonds. The adducts **1b** (B), **1b′** (C), **1c** (C) and **1c′** (F) (Table 4) turn out to represent the structures of maximum similarity with the transition state structure.

When maximum similarity adducts **1b** (B), **1b′** (C), **1c** (C) and **1c′** (F) (Table 4) are compared the following observations can be made: (1) the angle X–$C_{ald.}$–O_{OO} of **1c′** is smaller than that of **1b′** (indicating that in the case of branched **1′c** the formation of formate is more probable than in the case of straight chain **1′b**); (2) the difference of the values of the X–$C_{ald.}$–O_{OO} (X is the migrating group) angles is smaller in the case of **1c** and **1c′** than in that of **1b** and **1b′** [indicating that in the case of **1c/1c′** the probability of the reactions taking place along both pathways **a** and **b** (Fig. 1) could be higher than in the case of **1b/1b′**]; (3) the $O_{C=O}$–H_{OH} bond of **1c** (which should shorten in the reaction) is clearly longer than that of **1b**, **1b′** or **1c′** [indicating that the pseudo cyclic ring system of **1c** is less activated for the formation of acid (along pathway **a**, Fig. 1) than that of **1b**, **1b′** or **1c′**]; (4) the of O_{OH}–$C_{ald.}$ bond of **1b′** (which should shorten in the reaction) is clearly longer than that of **1b**, **1c** or **1c′** [indicating that the pseudo cyclic ring system of **1b′** is less activated for the formation of formate (along pathway **b**, Fig. 1) than that of **1b**, **1c** or **1c′**]; (5) the value of the X–$C_{ald.}$–O_{OO}–O_{OO} torsion angle of **1b′** deviates clearly more from 180° than that of **1b**, **1c** or **1c′** [indicating that the conformation of the migrating R group of **1b′** is less favorable for the reaction (formation of formate along pathway **b**, Fig. 1) than that of **1b**, **1c** or **1c′**]. These five observations indicate, that the formation of acid could be more favorable in the mixture containing **1b** and **1b′** than in that containing **1c** and **1c′** mainly because the competing reaction along pathway **b** (Fig. 1) is inhibited by unfavorable structural factors in the case of adducts of straight chain aldehydes such as **1b′**, respectively.

Conclusions

Results of this study indicate, that the 2-substitution of the reacting aldehyde appears to be crucial for formate production. A phenyl group at the α-position directed the reaction more efficiently to the corresponding formate than a straight chain group (2-phenylpropionaldehyde was converted almost completely to formate when *m*-CPBA was used as an oxidant). Under the typical conditions of O_2 in situ oxidation in chlorinated solvents 50% of the adduct formed from α-branched aldehydes, such as 2-ethylhexanal and 2-ethylbutanal, reacted via carbon chain migration. An even higher preference (e.g. 79/21 in the case of 2-ethylhexanal) for

Table 4. Maximum value of lengthening bonds (**L**) and minimum values of shortening bonds (**S**) of the 7-membered pseudo ring of the optimized structures of **1a**, **1b**, **1c** (equatorial H_{CHO}) and **1a′**, **1b′**, **1c′** (axial H_{CHO})

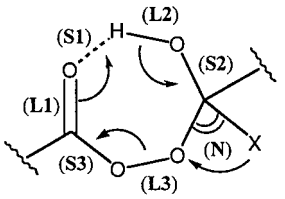

Struc.[a]	σ[b] (X–$C_{ald.}$–O_{OO})	max.**L1**[c] (C═O)	max.**S1**[c] ($O_{C=O}$–H_{OH})	max.**L2**[c] (O–H)	min.**S2**[c] (O_{OH}–$C_{ald.}$)	min.**L3**[c] ($C_{ald.}$–O_{OO})	min.**S3**[c] (O_{OO}–$C_{C=O}$)	γ[b] (X–$C_{ald.}$–O–O)
1b (B)	96.4	1.211	1.812	0.992	1.377[d]	1.468	1.345	176.5
1b′ (C)	102.2	1.211	1.810	0.993	1.382[e]	1.456	1.349[d]	172.5
1c (C)	96.3	1.212	1.826	0.993	1.378	1.465	1.346	177.1
1c′ (F)	100.9	1.212	1.819	0.994	1.379	1.457	1.349	176.4

[a] See Table 2.
[b] Values in degrees.
[c] Values in Å.
[d] Deviates from the minimum only by 0.001 Å.
[e] Deviates from the minimum only by 0.003 Å.

migration of the alkyl moiety was observed when *m*-CPBA was used as the oxidant. Cyclohexanecarboxaldehyde gave slightly less formate than open chain 2-ethylhexanal and 2-ethylbutanal.

In contrast to the behavior of α-branched aldehydes, both β-branched 3-methylbutanal and 3- phenylpropionaldehyde gave clean conversion to the corresponding acid, as did straight chain octanal and pentanal. Also Cinnamaldehyde and *trans*-2-decenal, in which the C=C double bond is conjugated with the aldehyde carbonyl, reacted through the acid route, even though their reactivity was poorer than that of the other aldehydes studied.

Computational studies on 12 conformers (of two epimers) of one linear and one α-branched peracid adduct **1** (total of 24 structures) indicate that there could be several minor factors which contribute to the formation of formate in the case α-branched aldehydes. Comparison of the conformers of adducts **1** of linear and α-branched aldehydes gives rise to a conclusion that in the case of linear aldehydes there are structural factors which hamper the formation of formate. In the case of adducts **1** of α-branched aldehydes, similar limitations were not observed.

Experimental

General

2-Ethylhexanal, 2-ethylbutanal, cyclohexanecarboxaldehyde, octanal, pentanal, 3-methyl propionaldehyde (Aldrich), 3-phenylpropionaldehyde, 2-phenylpropionaldehyde, cinnamaldehyde, *trans*-2-decenal (Fluka) and all the solvents were dried, distilled and preserved under inert atmosphere until use.

Gas chromatographic analyses were performed on a HP 6890 instrument: Polar Innowax column 30 m; initial column temperature 40°C; final column temp. 250°C; progress rate 10°C/min; constant flow 6.3 ml/min of carrier gas; initial pressure 0.93 bar. The main oxidation products of aldehydes were identified and quantified by comparison with authentic samples. Amount of 2-formylbutanal was quantified by using 3-formylheptanal (For preparation see below) as standard and amount of 2-phenylpropylformate by using 2-phenylpropanoic acid as standard. Decane or tetradecane was used as internal standard to calculate the exact amount of substance present in the reaction mixture.

The oxidation products were also identified by GC-MS. The sample components were identified using gas chromatography mass spectrometry in full scan mode and using electron impact (EI) and chemical ionization (CI). The EI spectra were identified by using the NIST-EPA-NIH Mass Spectral Library (version 1.5a) and manual interpretation. The CI spectra were used to confirm the molecular weight of an unknown in ambiguous cases.

The EI spectra were measured using HP Mass Selective detector infrared to HP 6890 Gas chromatograph. The MS scan range was *m/e* 25–500 and speed 1 scan/sec. The ion source temperature was 230°C and quadrupole temperature 150°C.

The CI spectra were measured using VG Prospec sector mass spectrometer interfaced to HP 5890 Series II Gas Chromatograph. The scan range was *m/e* 80–500 and scan speed 2 secs/decade. The ion source termperature was 200°C. Isobutene was used as reagent gas and the ion source pressure was maintained at 2×10^{-5} mbar by regulating the reagent gas flow. In both ionization cases, the GC columns and parameters were indentical to those of simple GC analyses. The GCMS interface was kept at 280°C and the electron multiplier voltage was adjusted to obtain proper sensitivity in both cases.

Oxidation of aldehydes. A flat-bottomed glass vessel equipped with condenser and oxygen balloon was charged with aldehyde, internal standard and solvent if used. Magnetic stirring (1000–1250 rpm) was commenced and the reaction mixture was evacuated and oxygenated three times at the chosen temperature. When reactions were done under air, the airflow in synthesis was 34 ml/min. In cases where overpressure was used, reaction was performed in a steel vessel.

Preparation of 3-heptylformate used as model compound. 3-Heptylformate was prepared from the corresponding alcohol (20 mmol) with dimethylformamide (20 mmol) and benzoyl chloride (20 mmol) in 12 ml dichloroethane according to the method of Barluenga et al.[8] Besides formate a small amount of unreacted 3-heptanol was present in the crude product. The formate was purified by vacuum distillation and the yield was 39%.

Acknowledgements

The TEKES foundation is acknowledged for partial financial support.

References

1. Reviews include: (a) McNesby, J.; Heller, C. *Chem. Rev.* **1954**, *54*, 325. (b) Sajus, L.; Roch, S. In *Comprehensive Chemical Kinetics*; Bamford, C., Tipper, C., Eds.; Elsevier: New York, 1980; Vol. 16, 89. (c) Maslow, S.; Bluymberg, E. *Russ. Chem. Rev.* **1976**, *45*, 155.
2. For example: (a) Godfrey, I.; Sargent, M.; Elix, J. *J. Chem. Soc., Perkin Trans. 1* **1974**, 1353. (b) Royer, J.; Beuglemans-Verrier, M. C. R. *Acad. Sc. Paris, Serie C* **1971**, 1818. (c) Camps, F.; Coll, J.; Messeguer, J.; Pericas, M. *Tetrahedron Lett.* **1981**, *22*, 3895.
3. DeBoer, A.; Ellwanger, R. *J. Org. Chem.* **1974**, *39*, 77.
4. Alcaide, B.; Aly, M.; Sierra, M. *J. Org. Chem.* **1996**, *61*, 8819.
5. Barrero, A.; Alvarez-Manzaneda, E.; Alvarez-Manzaneda, R.; Chahboun, R.; Meneses, R.; Aparicio, M. *Synlett* **1999**, 713.
6. Wavefunction, Inc. 18401 Von Karman Ave., Suite 370, Irvine, CA 92612, USA
7. Freccero, M.; Gandolfi, R.; Sarzi-Amade, M.; Rastelli, A. *J. Org. Chem.* **1999**, *65*, 2030.
8. Barluenga, J.; Campos, P.; Gonzales-Nunéz, E.; Asensio, G. *Synth. Commun.* **1985**, 426–428.